Microstructure–Property Linkage in Hybrid Laser–Arc Welded AHSS Plate

Link-Belt CRANES

COLLABORATORS
SSAB · SECAT
MECHACTION · WTTI
CLOOS · EVIDENT

Su Nayak, Troy Miller, Jeff Sparks

Link-Belt Cranes, Lexington, KY

*Corresponding author: snayak@linkbelt.com

AWS Professional Poster Competition · FABTECH 2026

1 PROBLEM & OBJECTIVE

Mobile-crane structures demand joints in **Strenx®-class advanced high-strength steel** (AHSS, YS ≥ 960 MPa) that retain both strength and −40 °C toughness under the low heat input of **hybrid laser–arc welding (HLAW)**.

Published HLAW work on 9 mm AHSS plate has not linked *through-joint microstructure, local mechanical response and volumetric flaw signatures* within a single qualified specimen — leaving no coherent basis for procedure qualification, NDE acceptance or structural-integrity assessment.

Objective: establish that linkage on one PQR-qualified 9 mm × 9 mm HLAW butt joint through a single multiscale chain — EBSD → nanoindentation → bulk tension & CVN → fractography → CT/PAUT.

2 MATERIALS & METHODS

Item	Specification
Base material	Strenx®-class AHSS, 9 mm plate; C 0.17, Mn 1.24, Si 0.22, Mo 0.59, V 0.039, Nb 0.014 wt.%; CE_IIW 0.55, CET 0.37
Process	Cloos QINEO GMAW arc-leading dual-beam fiber (4.5 kW core + 2.8 kW ring)
Filler / gas	Böhler Union NiMoCr (AWS ER100S-G), ⌀1.2 mm; 82 Ar – 18 CO_2
Heat input	0.79 kJ/mm; PB horizontal position; single pass, full penetration; PQR-255A
EBSD	FEG-SEM; 1000× (0.25 µm step) and 5000× (0.05 µm step); ODF via band-limited harmonics (L = 22)
Nanoindentation	Berkovich, 500 mN, 3 × 10 traverse; Oliver–Pharr + Nix–Gao ISE analysis (ISO 14577)
Bulk mechanical	Tension per AWS B4.0; CVN at −40 °C per ASTM A370 (7.5 × 10 mm sub-size)
Volumetric NDE	PAUT — Evident TFM/PCI (OmniScan X4); Lumafield Voyager CT (264 µm voxel)

3 HLAW PROCESS & TEST JOINT

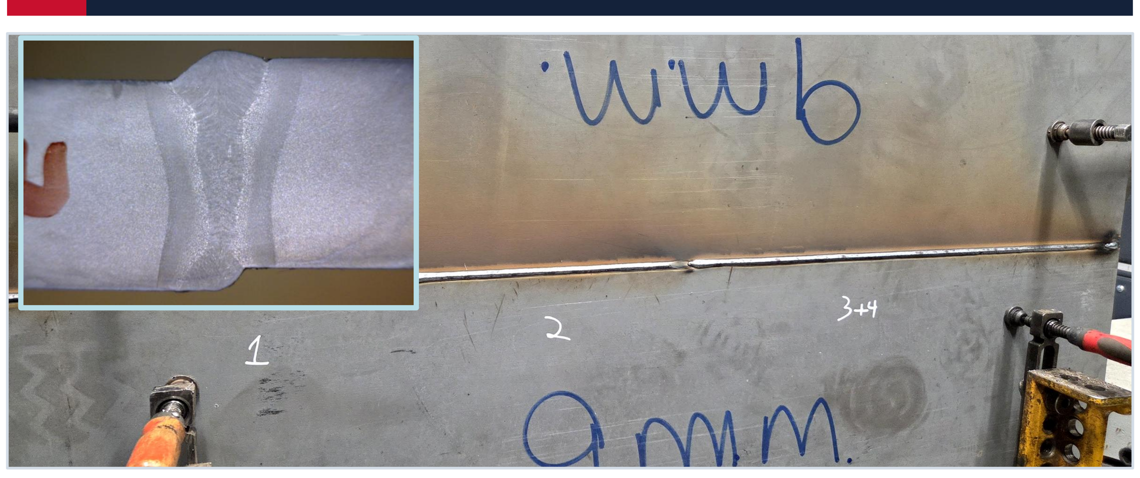

Fig. 1a Robotic HLAW butt weld on the 9 mm × 9 mm Strenx® test plate (plate 56) clamped in the Cloos cell, Haiger, Germany. Zero-gap square groove, single pass, arc-leading; positions 1–4 mark the downstream sectioning locations.

PROCESS PARAMETERS

Laser: dual-beam fiber, 4.5 kW core + 2.8kW ring
Arc pulsed GMAW, 227 A / 26 V, WFS 5 m/min
Travel 1.0 m/min · arc-leading · PB horizontal
Heat input 0.79 kJ/mm (η = 0.8)
Joint zero-gap square groove (nominal)
Preheat / PWHT none
HV max (HAZ), EN 1011-2 238

Fig. 1b Process-monitoring camera view of the hybrid weld pool: laser-induced vapour plume with the GMAW filler entering the leading edge of the common pool.

4 WELD MACRO & FZ GEOMETRY

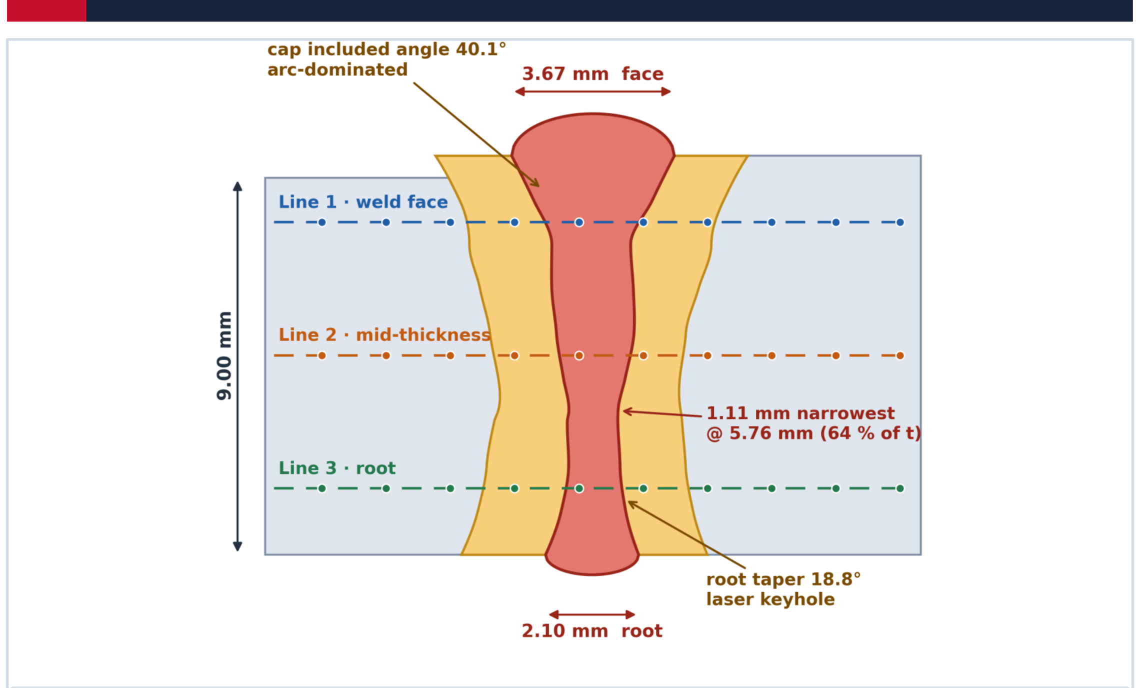

Fig. 2 Fusion-zone and HAZ boundaries traced from the calibrated macro-etch and scaled to the 9.00 mm plate thickness. The asymmetric hourglass profile separates the arc-dominated cap from the laser-keyhole root. Dashed lines mark the three nanoindentation traverses of Section 7.

Fusion-zone parameter	Value	Parameter	Value
Face-end width	3.67 mm	Cap included angle	40.1°
Root-end width	2.10 mm	Root taper angle	18.8°
Face : root ratio	1.75 : 1	Fusion-zone area	14.11 mm²
Narrowest section	1.11 mm	HAZ-only area	24.55 mm²
Depth of narrowest	5.76 mm (64 %)	Centreline shift	−0.02 mm

5 CROSS-SECTION EBSD (IPF ∥ ND)

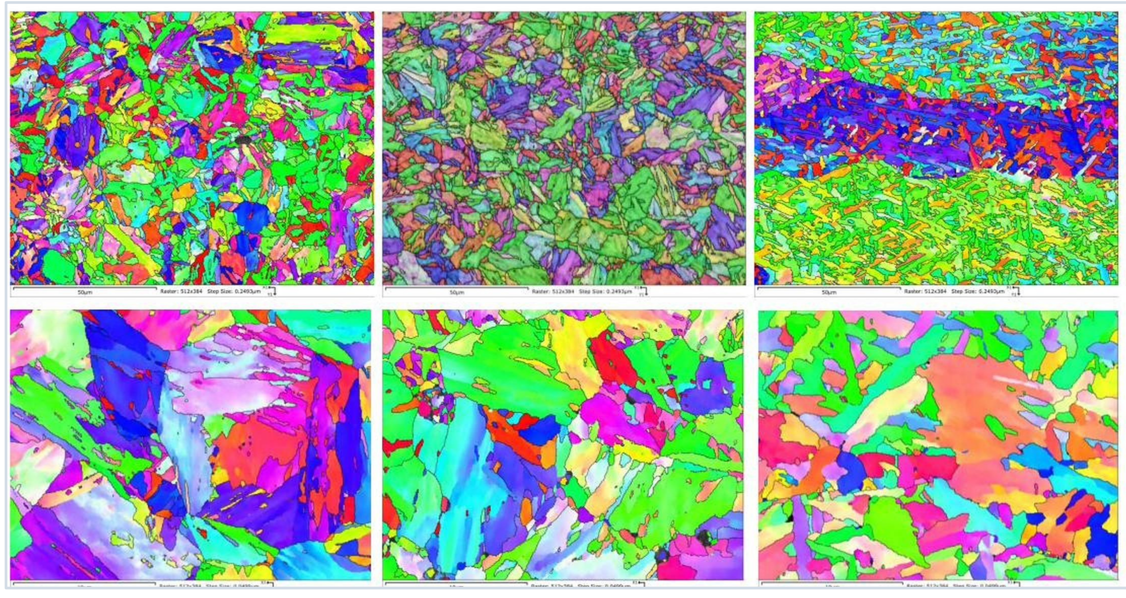

Fig. 3 Inverse pole figure (IPF ∥ ND) maps across the transverse cross-section: base metal → transition zone (1 mm from the fusion line) → weld centre. Top row 1000× (50 µm bar), bottom row 5000× (10 µm bar).

Base metal	Transition zone	Weld metal
Fine equiaxed structure, minimal preferred orientation	Directional rapid solidification — domains of preferred orientation	Equiaxed fine structure within domains of strong orientation
ECD 0.7 µm	ECD 0.7 – 2.4 µm	ECD 0.8 µm

Bulk texture & grain size (1000× fields)	ECD (µm)	m.u.d.	Texture index J
Base metal	2.5	1.68	1.22
1 mm from fusion line	2.3	2.10	1.34
Weld centre	2.4	3.63	2.70

6 WELD-FACE EBSD

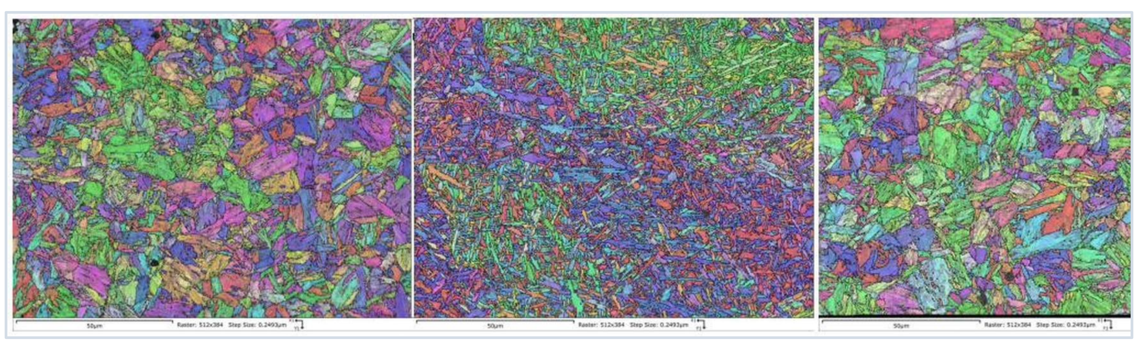

Fig. 4 Bulk-texture cross-check — weld-face IPF ∥ ND maps (1000×, 50 µm bar) on the milled weld-face plane of the 5 mm × 8 mm coupon: base metal → transition zone → weld metal.

Base metal	Transition zone	Weld metal
ECD 2.1 µm (SD 1.5)	ECD 1.7 µm (SD 0.9)	ECD 2.2 µm (SD 1.7)

- **Texture agrees between planes** — J ≈ 1.2 (BM) vs. 2.7 (WM); the joint is bulk-near-isotropic.
- **Grain refinement confirmed on a second plane** — no coarsening signature in the HAZ.
- **Elevated Fe_3C on the weld face** (1.3–4.2 % vs. < 0.3 % on the cross-section) is a milling-induced indexing artefact, not real cementite.
- **DIC-correlated post-tensile EBSD** at 7 sites (HAZ → FL → WM → FL → HAZ) showed progressive indexing fuzziness with local plastic strain, consistent with dislocation accumulation in the softer HAZ shoulders.

7 NANOINDENTATION TRAVERSE

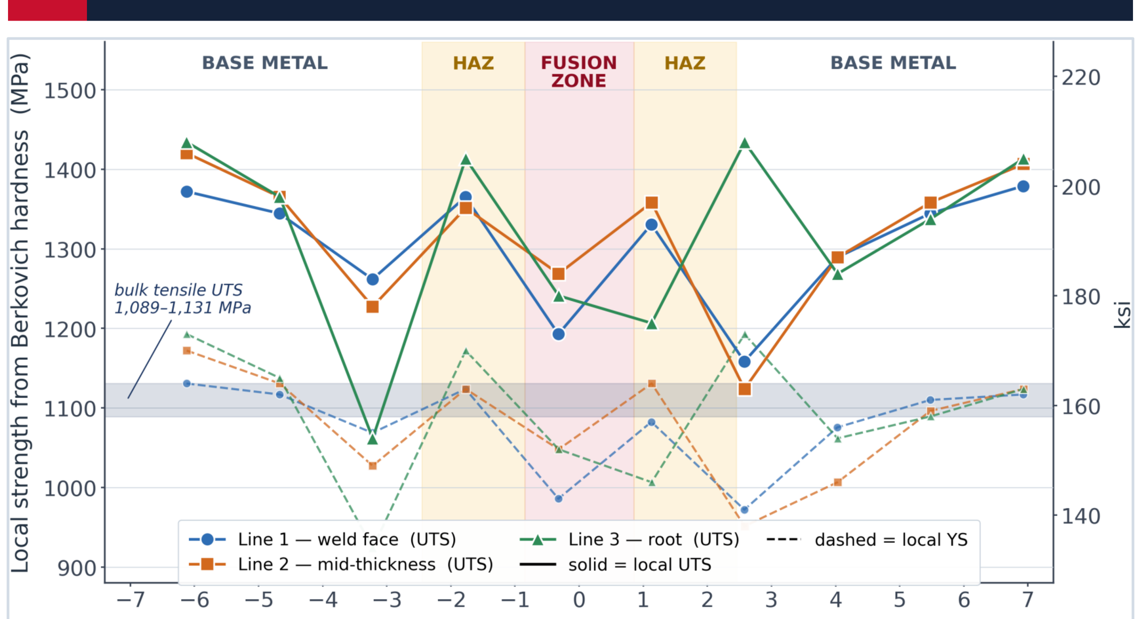

Fig. 5 Local UTS and YS derived from Berkovich hardness (500 mN, Oliver–Pharr) along three traverses through the 9 mm joint. Zone bands are taken from the traced macro geometry of Fig. 2.

- **Zone hardness** — WM 3.97 ± 0.24 GPa (n = 4), HAZ 3.98 ± 0.33 GPa (n = 6), BM 4.10 ± 0.32 GPa: indistinguishable within scatter.
- **No HAZ softening.** Local strength in weld metal and HAZ matches or slightly overmatches the parent plate.
- **Modulus E_{IT} ≈ 240 GPa** across all zones; fits power-law unloading.
- **Nix–Gao ISE** — the characteristic length h* is well defined in base metal and rises in the HAZ and fusion zone, indicating micron-scale microstructural heterogeneity.

8 BULK TENSILE (9 × 9 MM JOINT)

Specimen	UTS (MPa / ksi)	YS (MPa / ksi)	El (%)	RA (%)	Failure
Spec. 1	1 089 / 158	1 000 / 145	5.9	13.5	BM – ductile
Spec. 2	1 131 / 164	1 062 / 154	4.2	12.9	BM – ductile

Table 1 Both specimens fractured in the base metal in a ductile mode — the HLAW joint overmatches the parent plate in monotonic tension (WTTI Job #42007, AWS B4.0:2016).

9 CHARPY V-NOTCH IMPACT (−40 °C)

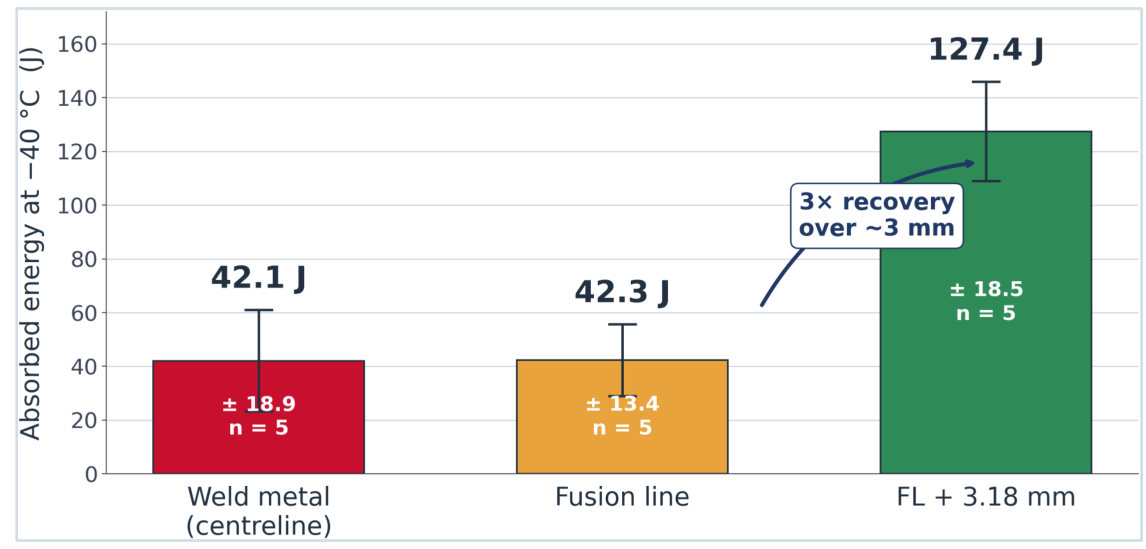

- **Sharp toughness recovery —** 42 J at the fusion line rises to 127 J only 3.18 mm away: a 3× step change across a band about one HAZ-width wide.
- **Weld-metal scatter (27.1 → 70.5 J, n = 5)** tracks solidification-mode heterogeneity resolved by fractography.
- **Design consequence —** the low-toughness band is narrow but real, and is the controlling feature for structural-integrity acceptance rather than the bulk tensile result.

10 SEM FRACTOGRAPHY

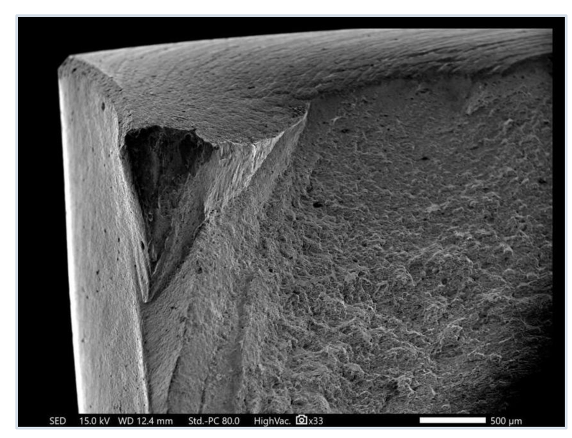

Fig. 6a Cup-and-cone corner of the tensile fracture, 33× SED (500 µm bar) — macroscopic ductile geometry.

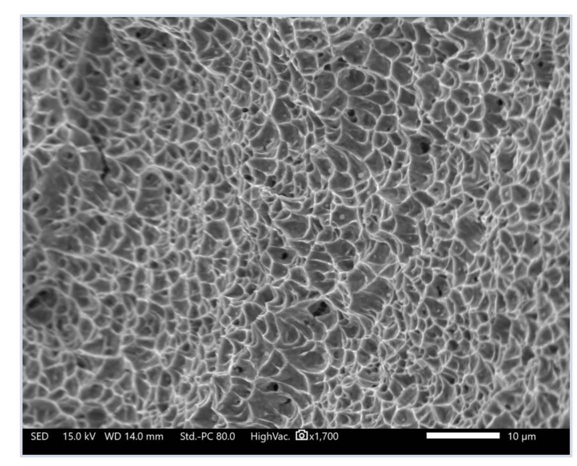

Fig. 6b Dimple field at 1 700× SED (10 µm bar) — uniform microvoid coalescence.

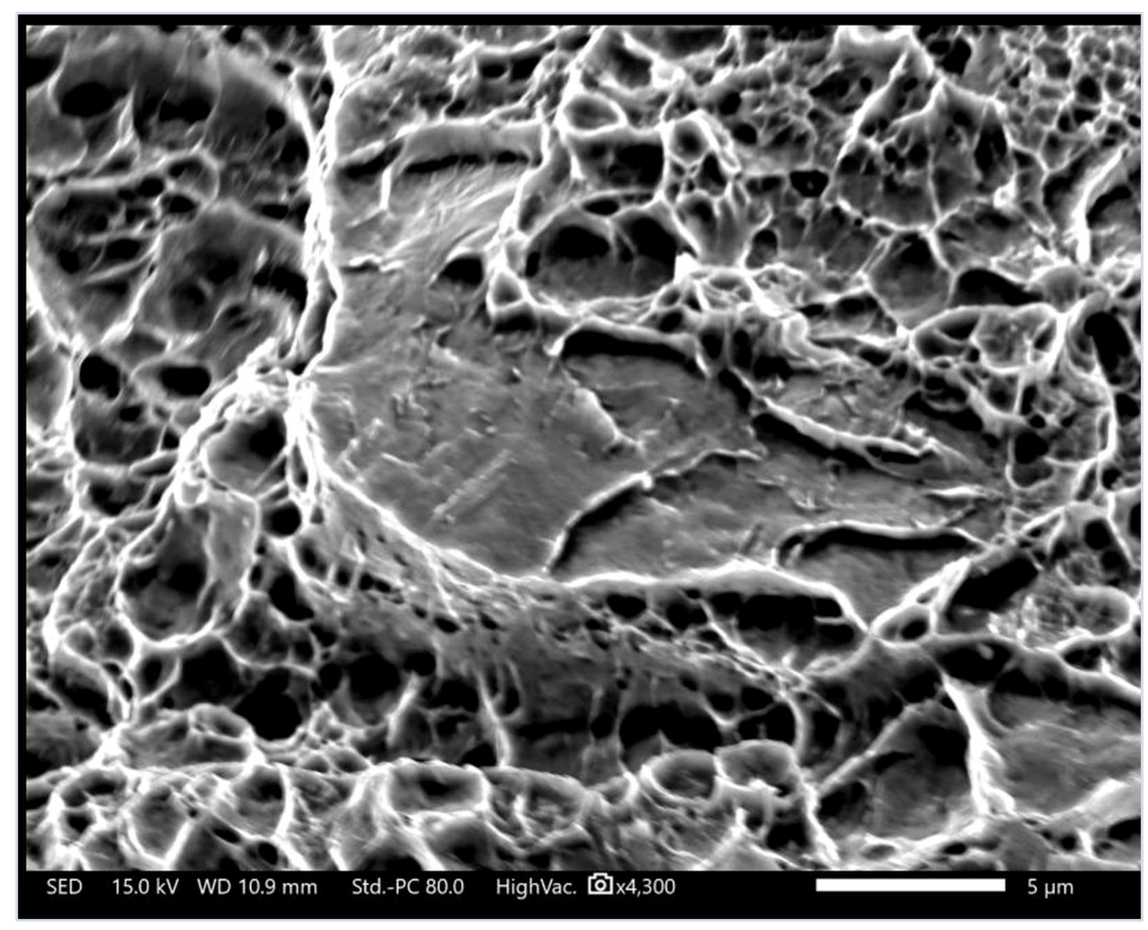

Fig. 6c Tensile fracture surface at 4 300× (SED, 15.0 kV, WD 10.9 mm). Equiaxed 5–10 µm dimples characteristic of microvoid coalescence in HSLA steel; the central island is nucleated at an elongated MnS / oxide inclusion (5 µm bar).

11 VOLUMETRIC NDE — CT + PAUT

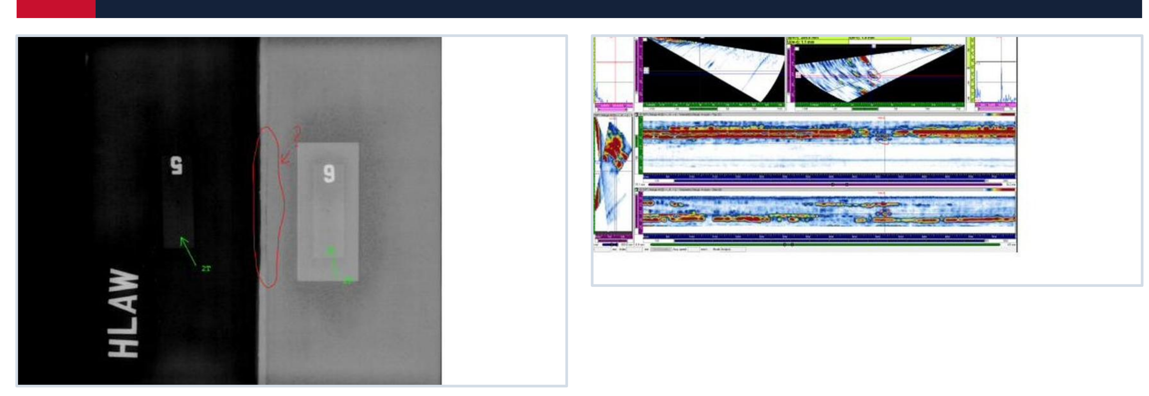

Fig. 7 Volumetric NDE of the coupon family. Left: Lumafield Voyager CT slice (264 µm voxel) — the circled sub-millimetre indication lies near the fusion line. Right: Evident PAUT TFM/PCI (OmniScan X4, 10L32-A10) volumetric merge — the same indication resolved at ~1.1 mm depth.

12 KEY OUTCOMES & DISCUSSION

- **UTS 1089-1131 MPa, YS 1000-1062 MPa** — both specimens failed BM-ductile.
- **CVN −40 °C:** WM 42.1±18.9 J | FL 42.3±13.4 J | FL + 3.2 mm 127.4±18.5 J.
- **Texture J 1.22 (BM) → 1.34 (1 mm FL) → 2.70 (WM);** ECD 2.3 – 2.5 µm preserved across the joint.
- **Zone hardness constant within scatter:** WM≈HAZ≈BM (Berkovich, 0.5 mN).
- **The HLAW thermal cycle preserves parent-plate grain refinement;** Ti/V/Nb carbonitrides pin the HAZ (Bhadeshia & Honeycombe, 2017).
- **Bulk texture is modest and near-isotropic;** the elevated 5000× J-index reflects Kurdjumov–Sachs variant clustering within prior-austenite blocks rather than a genuine macrotexture.
- **CVN scatter maps to acicular-ferrite / upper-bainite islands** resolved by SEM fractography of the lowest-energy weld-metal specimens.

CONCLUSIONS

1. Multiscale characterisation of a single qualified 9 mm HLAW joint establishes a coherent microstructure–property linkage: a fine-grained (ECD ≈ 2.4 µm) low-transformation-temperature product across all zones, with only moderate solidification texture (J = 2.70) at the fusion-zone centre.
2. The joint overmatches the parent plate in tension (UTS 1 089 – 1 131 MPa, BM-ductile failure) and shows a sharp CVN recovery from 42 J at the fusion line to 127 J just 3.18 mm away — a narrow but critical low-toughness band that governs structural-integrity acceptance.
3. Volumetric NDE (Lumafield CT + Evident PAUT TFM/PCI) resolves sub-millimetre indications on the coupon family and is directly correlatable with the destructive dataset — an end-to-end qualification workflow for HLAW of AHSS crane structures.

ACKNOWLEDGMENTS

Dan Keener and Richard Shultz (Link-Belt Cranes); Magnus Carlsson and Mikael Reinberth (SSAB AB); Cloos Schweisstechnik (Haiger, Germany); Ryan Teer (Evident Scientific — TFM/PCI); Shridas Ningileri and Nick Nanninga (Secat); WTTI (bulk mechanical testing).